Cerebral Cortex August 2010;20:1964–1973
doi:10.1093/cercor/bhp268
Advance Access publication December 24, 2009

Sensitivity of Human Visual and Vestibular Cortical Regions to Egomotion-Compatible Visual Stimulation

Velia Cardin and Andrew T. Smith

Department of Psychology, Royal Holloway, University of London, Egham, Surrey TW20 0EX, UK

The analysis and representation of visual cues to self-motion (egomotion) is primarily associated with cortical areas MST, VIP, and (recently) cingulate sulcus visual area (CSv). Various other areas, including visual areas V6 and V6A, and vestibular areas parietoinsular vestibular cortex (PIVC), putative area 2v (p2v), and 3aNv, are also potentially suited to processing egomotion (in some cases based on multisensory cues), but it is not known whether they are in fact involved in this process. In a functional magnetic resonance imaging (fMRI) experiment, we presented human participants with 2 types of random dot kinematograms. Both contained coherent motion but one simulated egomotion while the other did not. An area in the parieto-occipital sulcus that may correspond to V6, PIVC, and p2v were all differentially responsive to egomotion-compatible visual stimuli, suggesting that they may be involved in encoding egomotion. More generally, we show that the use of such stimuli provides a simple and reliable fMRI localizer for human PIVC and p2v, which hitherto required galvanic or caloric stimulation to be identified.

Keywords: egomotion, fMRI, human V6, PIVC, vestibular, visual

Introduction

Optic flow provides an important visual cue to the estimation of self-motion (egomotion; Gibson 1950; Warren et al. 1988). However, in the mammalian brain, vestibular and somatosensory signals are integrated with visual information to compute egomotion parameters. In macaques, there is much evidence that areas MST and VIP are involved in encoding visual cues for egomotion and are also sensitive to vestibular and somatosensory cues (e.g., Saito et al. 1989; Duffy and Wurtz 1991a, 1991b, 1995). Cells in the dorsal portion of area MST (MSTd) respond preferentially to specific optic flow components (expansion, contraction, and rotation; Duffy and Wurtz 1991b) and are sensitive to the direction of heading in the visual and vestibular domains (Duffy and Wurtz 1995; Page and Duffy 2003; Gu et al. 2006, 2007, 2008). In polysensory area VIP, neurons have visual properties similar to MSTd (Schaafsma and Duysens 1996) but are even more sensitive to motion in the vestibular and somatosensory modalities (Duhamel et al. 1998) and many response fields are in craniocentric coordinates (Zhang et al. 2004).

Vestibular regions also contribute to the processing of egomotion. Macaque anterior parietal cortex contains 2 sensory regions that are primarily regarded as vestibular but also receive visual and somatosensory information (see Guldin and Grüsser 1998, for review). These are parietoinsular vestibular cortex (PIVC), in the posterior insula and adjoining parietal cortex, and area 2v, in the postcentral sulcus. These areas, together with area 3aNv, in frontal area 3a, are potentially suited to integrating multisensory cues (including optic flow) in the processing of egomotion.

In humans, sensitivity to heading direction has been shown in MT+ and a posterior region in the dorsal intraparietal sulcus (DIPSM/L; Peuskens et al. 2001). Studies of egomotion have shown differential responses to egomotion-compatible (EC) optic flow in putative area VIP (pVIP), MST, and to a lesser extent in V5/MT and also in the cingulate sulcus visual area (CSv; Wall and Smith 2008). Differential responses to vection—the illusion of egomotion induced by optic flow—have been shown in further parieto-occipital regions and dorsal intraparietal sulcus (Brandt et al. 1998; Kovács et al. 2008), but the identities and roles of these regions have not been determined. In contrast, deactivations have been observed in PIVC during periods of vection (Brandt et al. 1998; Kleinschmidt et al. 2002). The same result is observed in PIVC with optokinetic stimulation (Dieterich, Bense, Stephan, et al. 2003; Kikuchi et al. 2009).

Summarizing, a network of visual and multisensory cortical regions including MST, regions in the intraparietal sulcus and CSv have been shown to be involved in processing visual cues for egomotion in humans. However, involvement has not been established for other cortical visual regions, in particular those located in the parieto-occipital sulcus (POS) (V6 and V6A) or for various regions that are primarily vestibular but may receive visual input, such as area 2v.

Area V6 is located in the POS of macaque and humans (Galletti et al. 1991, 1996; Galletti, Fattori, Kutz, et al. 1999; Pitzalis et al. 2006). In macaque, V6 abuts the end (the representation of the far periphery) of areas V3 and V3A. It has a clear retinotopic organization, representing the contralateral hemifield, most of its cells are visually responsive, and about 75% are direction sensitive, suggesting that V6 plays a part in visual motion processing. Adjacent area V6A, which occupies the dorsal/anterior portion of the sulcus, has no obvious retinotopic organization and only about 60% of the neurons are visually responsive. Visual neurons are again predominantly motion sensitive. It has been suggested that macaque V6 and V6A have a pivotal role in providing visual motion information to the motor system (Galletti et al. 1991, 1996; Fattori et al. 1992; Galletti, Fattori, Gamberini, et al. 1999).

In humans, V6 has been identified using wide-field (110°) retinotopic mapping (Pitzalis et al. 2006). This region is similar to macaque V6 in terms of its retinotopic organization and its position with respect to V3 and V3A. Human V6 is confined to the dorsal portion of the POS, occupying the fundus and posterior bank of the sulcus; it contains a complete representation of the contralateral hemifield, with the lower field located medially and more anterior to V3/V3A, extending

dorsally to the upper field. Recent work by Pitzalis et al. (2009) has shown that, as in primates, human V6 is a motion area, responding much more strongly to coherent than incoherent motion. However, it is not clear if this area responds to coherent global motion in general, such as that arising from a flock of birds or movements of waves or (like VIP and CSv) is selective to flow fields that are likely to reflect egomotion.

The macaque PIVC is one of several major cortical areas that respond well to vestibular stimuli and the most prominent in terms of the proportion of neurons that are responsive to such stimuli (Grüsser et al. 1990a; see Guldin and Grüsser 1998 for review). In area PIVC, two-thirds of neurons respond to vestibular stimulation; these show different optimum sensitivities to different planes of rotation, collectively representing all possible rotation planes, in head-centered coordinates (Grüsser et al. 1990a). Most of the neurons in this region that respond to vestibular stimulation are also sensitive to optokinetic stimulation, with some cells showing the strongest responses to visual stimulation in the direction that gives the maximum vestibular response and others showing maximal responses to stimulation in the opposite direction (Akbarian et al. 1988). Neurons in macaque 2v are also sensitive to vestibular and optokinetic stimulation (Büttner and Buettner 1978; Büttner and Henn 1981). Human PIVC has also been identified and is one of the most strongly activated regions during galvanic or caloric vestibular stimulation (Bucher et al. 1998; Lobel et al. 1998; Fasold et al. 2002). Other regions of the macaque brain known to have vestibular afferents include area 7, 3aNv, 2v, and visual posterior sylvian (VPS). Knowledge of the functional differences among these areas is limited, even in macaques. It has been suggested that PIVC is a core region, responsible for generating a unified percept of "head-in-space" (Guldin and Grüsser 1998), but these areas have received much less attention than visual cortical regions and much remains to be understood. In humans, it has been shown that multiple regions respond to vestibular stimulation (Bucher et al. 1998; Lobel et al. 1998), but the interrelations of these regions are even less well understood than in macaques.

It is thought that all macaque vestibular areas are polysensory and many have visual input (Guldin and Grüsser 1998; Brandt and Dieterich 1999). This suggests that visual and vestibular information may be combined in these areas for perception and control of posture and movement. Specifically, it is possible that some of them are, like MSTd (Duffy and Wurtz 1995; Page and Duffy 2003; Gu et al. 2006, 2007, 2008), involved in combining or comparing visual and vestibular cues to egomotion.

In the present study, we wanted to explore the sensitivity of various visual and vestibular areas in the processing of visual cues to egomotion. The sensitivity of area V6 to optic flow stimulation, in addition to its large receptive fields and its connections to MST and VIP, makes this area potentially suited, but it is not known whether it is, indeed, involved in such processes. Similarly, the multisensory nature of areas processing vestibular signals suggests that they too might be integrating visual cues in the computation of egomotion, but this has not been demonstrated directly. We have conducted an fMRI experiment using a wide visual display (58°) of moving dots with a flow structure that was either compatible or incompatible with egomotion (Wall and Smith 2008). Our results revealed that putative area V6 (pV6), PIVC, and putative area 2v (p2v) are all differentially sensitive to egomotion-compatible flow, suggesting that they may be involved in computing egomotion.

Materials and Methods

Main Experiment

Eleven individuals (10 women, including one of the authors, age 18–32 years), with normal or corrected-to-normal vision, gave written consent to participate in this study, which was conducted in accordance with the Declaration of Helsinki and approved by the local ethics committee at Royal Holloway, University of London. Standard MRI screening procedures were followed for all participants, and naive volunteers were paid for their participation.

The stimuli consisted of 800 moving dots arranged in an EC or egomotion-inconsistent (EI) pattern, as described elsewhere (Wall and Smith 2008). The EC condition consisted of a 58° × 58° square field of dots moving in a coherent optic flow pattern containing expansion/contraction and rotation components that varied over time, consistent with self-motion on a varying spiral trajectory (Morrone et al. 2000), displayed at 60 fps. For a given dot with radius r, angle θ and local speed v, its trajectory was defined by:

$$dr/dt = v\cos\phi \quad (1)$$

$$d\theta/dt = (v\sin\phi)/r. \quad (2)$$

Radial and angular velocities are defined by dr/dt and $d\theta/dt$, respectively. The direction of optic flow was defined by ϕ, which varied over time from $-\pi$ to π generating a stimuli with radial, circular, and spiral motion. The local speed did not vary with distance from the origin to avoid local speed confounds between the EC and EI stimuli (pilot fMRI results show that responses are similar for 1) stimuli with constant speed and size and 2) stimuli with radially increasing speed and size).

The EI stimulus consisted of a 3 × 3 array of 9 identical panels, each containing a smaller version of the EC stimulus. Although the individual panels contain optic flow, the overall pattern is not consistent with egomotion because flow induced by observer motion can have only one center of motion. In true optic flow stimuli, the size and speed of motion of the features in the image increase with eccentricity. Because the introduction of these scaling factors would result in different distributions of dot size and speed in our 2 stimuli, and potentially spurious results, we kept the dot size, dot speed, and number of dots in the whole array identical across conditions in order to equate low-level visual characteristics. As a result, our stimulus does not resemble "true" optic flow in terms of the scaling of size and speed with eccentricity typical of motion through a cloud of dots. The use of time-varying flow ensured that all locations were stimulated by all dot directions during the course of the stimulus cycle. It also gives larger response than (say) continuous expansion, perhaps, because multiple flow-sensitive neurons are stimulated. It also ensures that adaptation at any one local direction is minimal.

Each stimulus was presented for 3 s in an event-related design, with intertrial intervals (ITIs) in which the screen was blank (apart from a central fixation spot). The ITIs varied between 2 and 10 s, following a Poisson probability distribution. A scanning session consisted of 6 experimental runs, the order counterbalanced across participants. Each run had 32 trials (16 per condition) presented in a pseudorandom order, plus 10 s at the beginning and the end, lasting in total 4 min 48 s. Participants were instructed to fixate a small (2°) central square that changed color throughout the run at a rate of 2.5 Hz. To ensure fixation and to minimize fluctuations in attention, they performed a task that consisted of counting the number of instances of a particular color. The stimuli were generated using OpenGL libraries in C++ and projected into a screen using an LCD projector. To obtain wide-field visual stimulation, emulating natural optic flow, the screen was viewed via a custom optical device that magnified the image. The device was monocular and was positioned over the participant's preferred eye; the unstimulated eye was occluded. In 4 of the participants, the experiment was repeated in a separate, later scan, with the same

projection stimulus seen in binocular free view via a mirror, which reduced the retinal image size to 20°.

Images were acquired with a 3T MR scanner (Magnetom Trio; Siemens, Erlangen, Germany) equipped with a custom 8-channel posterior-head array head coil (Stark Contrast, Erlangen, Germany). Functional images were acquired with a standard gradient-echo, echo-planar sequence (time repetition [TR] = 2500 ms, time echo [TE] = 31 ms, flip angle = 90°, voxel size = 3 × 3 × 3 mm, 35 axial slices, bandwidth = 1396 Hz/pixel). For coregistration purposes, at the beginning of each scanning session, we also acquired 2 single-volume echo-planar imaging (EPI) sequences that had the same position parameters as the experimental runs: one using the scanner's integral whole-body coil (BC) to give uniform contrast and another immediately after, acquired with the posterior array (PA) head coil.

For each participant, we also acquired a high-resolution T_1-weighted 3-dimensional (3D) anatomical image (modified driven-equilibrium Fourier transform [MDEFT; Deichmann et al. 2004], 176 axial slices, in-plane resolution 256 × 256, 1-mm isotropic voxels, TR = 7.92 ms, TE = 2.45 ms, flip angle = 16, bandwidth = 195 Hz/pixel) using a standard (whole head) Siemens 8-channel head coil. MDEFT was chosen in place of standard 3D anatomical sequences because of its improved contrast between gray matter and white matter, which is beneficial for segmentation and flattening. This anatomical image was used as a reference to which all the functional images were coregistered.

All data were preprocessed and analyzed with BrainVoyager QX (version 1.10; Brain Innovation, Maastricht, the Netherlands). EPIs were corrected for head motion and slice timing and were filtered with a temporal high-pass filter of 0.01 Hz. No smoothing was applied. All functional images were aligned to the PA-EPI acquired at the beginning of the scan session. Due to the steep posterior-to-anterior gradient of the EPIs acquired with the posterior array head coil, coregistration of these images to the anatomy is poor. Therefore, we coregistered the BC-EPI to the MDEFT and assumed no head movements between the acquisition of this image and the PA-EPI. Coregistration accuracy was checked visually.

Analysis was conducted by fitting a general linear model (GLM) with regressors representing the 2 stimulus categories and 6 movement parameters. For every experimental condition, each stimulus presentation was modeled as a boxcar of 3-s duration, convolved with a canonical hemodynamic response function and entered into a multiple regression analysis to generate parameter estimates for each regressor at every voxel. Movement parameters were derived from the realignment of the images and included in the model. The first 3 volumes of each run were discarded to allow for T_1 equilibration effects. Correction for effects of serial autocorrelations was applied using the first-order autoregression AR(1) method. Appropriate contrasts were defined individually for each participant and the results visualized using flattened or inflated representations of each person's MDEFT.

All images were aligned to the AC-PC axis (anterior to posterior commissure), and all analyses were performed and are presented, in this orientation. To obtain the coordinates of each region of interest (ROI) in a normalized anatomical space, all data were subsequently transformed to Talairach and Tornoux space using BrainVoyager QX.

Effect sizes (beta values) were extracted from several ROIs by averaging across all voxels in the ROI to compute the ratio of the response magnitudes for EI and EC stimuli. For Figure 3*B*, beta values were extracted from 2 independently defined ROIs (V3A and V6) obtained with retinotopic mapping (see below). In the case of Figure 6, beta values were extracted from ROIs defined separately in each hemisphere with the statistical contrast (EC–EI) using as a cutoff threshold the highest P value which resulted in at least 40 contiguous activated voxels.

Retinotopic Mapping

Retinotopic mapping was performed to demarcate areas V1–V4 and, where possible, V6. Standard retinotopic mapping procedures were used (Engel et al. 1994; Sereno et al. 1995). Two stimulus runs were performed in a separate scanning session, conducted with binocular viewing via a standard mirror. In each run, a counterphasing checkerboard "wedge" stimulus (a 24° sector) rotated clockwise at a rate of 64 s/cycle (8 cycles per run). The counterphase frequency was 8 Hz and the rotating wedge covered an area 24° visual angle in diameter. Check size was scaled by eccentricity in approximate accordance with the cortical magnification factor. Stimuli were projected in the same way as in the main experiment. Images were acquired and preprocessed as in the main experiment, but in this case, volumes consisted of 28 slices and TR = 2000ms. In 6 participants, a second retinotopic map was subsequently derived based on additional scans employing a wide-field (70° dm) version of the wedge stimulus presented monocularly with the optical device used for the main experiment (previous section).

Data were analyzed by fitting a model to the time course obtained with the rotating wedge stimulus. This consisted of a rectangular wave of duty cycle 24/360, reflecting the duration of stimulation at any portion of the visual field, convolved with the HRF. The phase of the fitted response was taken as an index of visual field location, in terms of polar angle. Reversals of the direction of phase change across the cortical surface were taken as boundaries of visual areas. The boundaries of visual areas V1–V4 were drawn by eye, on the basis of these reversals viewed on a flattened version of each participant's reference anatomy. V6 was defined with reference to the description provided by Pitzalis et al. (2006); we looked for a complete hemifield representation close to the peripheral visual field representations of V2, V3, and V3A. The flattened representation of each hemisphere was created by segmenting and reconstructing the border between gray and white matter within each hemisphere of the MDEFT scan using BrainVoyager. The resulting surfaces were smoothed, inflated, and cut along the calcarine sulcus. Finally, the surface was flattened and corrected for linear distortions.

Results

To localize areas that are selectively responsive to EC stimuli, we measured the difference between the responses to the 1-patch and 9-patch stimuli, estimated by performing the statistical contrast (EC–EI). The analysis was performed separately for each individual. The rationale behind this approach is that a cortical area that encodes information relevant for egomotion will be active primarily in response to global motion patterns that have a unique centre of flow and might have arisen from movement of the observer (EC stimuli). In contrast, brain regions that process global flow irrespective of context or, indeed, those that process only local motion should respond well to both EC and EI stimuli since both have local motion and both have a global motion structure. Contrasting one response against the other isolates areas with differential sensitivity.

We have previously shown (Wall and Smith 2008) that this comparison identifies at least 2 regions as differentially sensitive to EC stimuli: pVIP and a little-studied visual area which we refer to as CSv. MST is also sensitive, to a lesser extent. The present results confirm these findings, showing bilateral activity in the cingulate sulcus (Fig. 1, circled light blue) and the anterior fundus of the intraparietal sulcus (Fig. 1, yellow; Fig. 5). These regions correspond to CSv and putative VIP, respectively. CSv was identified in 21/22 hemispheres (Table 1; mean Talairach coordinates: x = 11, y = –25, z = 40 [right]; x = –10, y = –23, z = 39 [left]); and pVIP was localized in 19/22 hemispheres (Table 1; right: x = 26, y = –56, z = 48; left: x = –25, y = –55, z = 50). A cluster in the MT complex was observed in 20/22 hemispheres (Fig. 1, pink, and Table 1; right: x = 39, y = –60, z = 1; left: x = –39, y = –62, z = 5). This area could correspond to MST since Wall and Smith (2008) have shown that MST shows at least a degree of preference for a single flow stimulus. However, a full independent characterization of MT and MST would be necessary to confirm this claim. Therefore, here we refer to this activation simply as MT+.

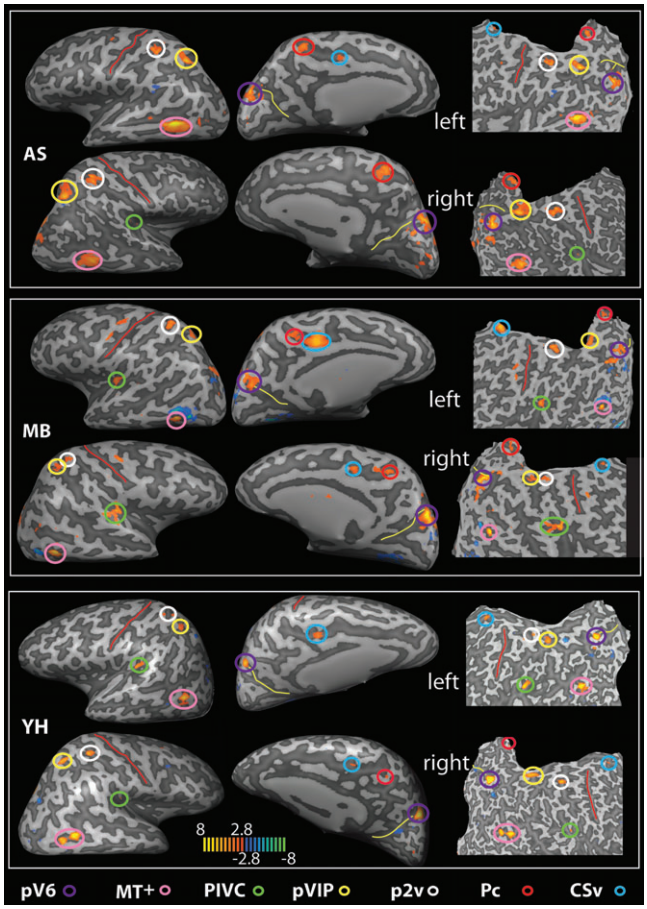

Figure 1. Brain areas selectively responsive to the egomotion-compatible (EC) stimulus. For 3 participants (AS, MB, and YH), the map of regions showing a significantly greater response to one flow stimulus than to an array of flow stimuli is overlaid onto inflated (left and central panels in each case) and flattened (right panels) representations of the left and right hemispheres. *T* values are color coded (see color bar). Various active regions are highlighted by colored circles (see color key; all activations shown thresholded at $P < 0.005$ uncorrected). The red line marks the central sulcus and the yellow line the POS. Pc, precuneus.

In addition, results from the contrast (EC–EI) revealed significant bilateral activations across participants in 4 further regions (see Table 1 and Fig. 1) that were not identified in the less comprehensive study of Wall and Smith (2008). These were

(i) the dorsal margin of the POS (Figs 1 and 2, purple),
(ii) the posterior insula, at the junction with the parietal operculum (Figs 1 and 4, green),
(iii) the superior parietal lobule, in the dorsal margin of the postcentral sulcus (Figs 1 and 5, white), and
(iv) the precuneus, in the ascending ramus of the cingulate sulcus (Figs 1 and 5, red).

Results for these regions are described in more detail below.

Parieto-occipital Sulcus: pV6

Our data show, consistently across all hemispheres, a region selectively responsive to EC stimuli in the dorsal margin of the POS, with mean Talairach coordinates: $x = 14$, $y = -77$, $z = 30$, and $x = -11$, $y = -79$, $z = 30$ (Fig. 2*A* and Table 1). To identify the location of this region in relation to the well-established retinotopic areas, we retinotopically mapped and identified visual areas V1–V7 in all our participants. The continuous black line in Figure 2*B* (upper panels) shows, for 3 participants, the location of the voxel cluster in the POS with respect to retinotopic visual areas. The lower panels in Figure 2*B* show the thresholded activation from the contrast (EC–EI), from which the black outline is derived, overlaid onto the same flattened representations. In these and all our participants, the voxel cluster in the POS is located medial to V3A (see Supplementary Fig. 1 for more examples). The location of this activation could correspond to the definition of human V6 of Pitzalis et al. (2006), and it coincides with the coordinates of the location of V6 that they report ($x = 9$, $y = -78$, $z = 37$). Our coordinates are also in agreement with earlier, less detailed reports of a human V6 complex (de Jong et al. 2001; Simon et al. 2002). However, even though we observed flow-related activity in the POS for all the hemispheres we analyzed (Fig. 2 and Table 1; Supplementary Fig. 1), a clear demarcation of V6 was difficult to obtain with our standard retinotopic mapping procedure (12° radius wedge in free view): we were only able to demarcate V6 in 5/22 hemispheres (See Supplementary Fig. 1*a*,*d*,*g*,*m*, for some examples). In their study, Pitzalis et al. (2006) emphasized the need for a wide-field mapping stimulus due to the lack of magnification of the central visual field relative to the periphery in V6 (Galletti, Fattori, Gamberini, et al. 1999). We therefore conducted further retinotopic mapping in 6 participants, with a 60° field. The results are shown in Figure 3*A* and Supplementary Figure 1. In 8 of the 12 hemispheres, we could see a hemifield representation medial to V3A (outlined with a thick red line in Fig. 3*A* and Supplementary Fig. 1), with the upper field located more medially and closer to the peripheral visual field representation of V2 and V3 than the lower field, which was located more superiorly and laterally. Figure 3*A* and Supplementary Figure 1 show that the overlap between this retinotopically defined region and the differential activation to EC stimulation in the POS was good in 7 of the 8 cases.

The location of the hemifield map was rather variable. In some cases (including Fig. 3*A*, right panel), it corresponded well to V6 as described by Pitzalis et al. (2006), being located in the posterior branch of the POS (where present) and abutting V2, V3, and V3A. In other cases (e.g., Fig. 3*A* left panel), it appeared in a slightly more dorsal/anterior location, closer to V7 than V3. When this occurred, correspondence between the retinotopic hemifield and the EC flow-related activity remained good, and there was no other competing hemifield map closer to V3. Therefore, it seems likely that the area identified is functionally the same in all hemispheres, despite some variability in its anatomical position. Nonetheless, the variable location raises some doubt as to whether the area corresponds to area V6 of Pitzalis et al. (2006). We return to this question in the Discussion and meanwhile refer to the area as pV6.

To quantify the differential sensitivity of area pV6 to EC visual stimulation, we extracted the beta values estimated for each condition in all the voxels of this area as defined retinotopically. We calculated the mean beta values across all voxels in the ROI, for each stimulus condition. We then computed the ratio of the means (EC–EI) for the ROI and averaged the result across hemispheres. An EI/EC coefficient of 1 means that EI and EC have the same effect in a given ROI, whereas a value of 0 will mean that EI had no effect. As a comparison, we did the same analysis in area V3A, which is

Table 1
ROIs Talairach coordinates

	Subject	pV6			PIVC			p2v			pVIP			Pc			CSv			MT+		
		x	*y*	*z*	*x*	*y*	*z*	*x*	*y*	*z*	*x*	*y*	*z*	*x*	*y*	*z*	*x*	*y*	*z*	*x*	*y*	*z*
Left	AS	−8	−87	29	—	—	—	−28	−46	43	−26	−60	43	−13	−53	50*	−10	−21	38*	−41	−60	0
	EC	17	−86	28	−38	−29	18	−29	−43	47*	—	—	—	−15	−41	42	−12	−27	36	−36	−60	−1
	JC	−15	−82	28	−41	−33	19*	−23	−43	62	−23	−56	49	—	—	—	−4	−31	42	−39	−66	5
	JS	−17	−75	30	−40	−32	19	—	—	—*	−23	−48	54	−8	−42	50*	−9	−19	45*	—	—	—
	KL	−23	−77	34	−37	−28	18*	—	—	—	−28	−49	48	−13	−51	52	−13	−26	42	−39	−58	7
	MB	−8	−76	36	−35	−25	18	−29	−39	54	−21	−60	55	−10	−42	50	−12	−21	37	−37	−58	3
	MN	−14	−76	27	—	—	—	−20	−40	47*	−27	−55	52*	−20	−40	47	−10	−19	39**	−40	−64	4
	PK	−18	−79	29	−36	−34	23	−26	−46	52	−27	−58	57*	−13	−40	45**	−11	−24	40*	−37	−58	6
	SD	−11	−77	21	−36	−29	21*	−28	−43	52*	—	—	—	−15	−51	48*	−11	−24	40	−40	−67	3*
	VC	−7	−78	29	−35	−39	15	−27	−49	48	−21	−62	45*	−15	−56	47	−9	−23	32	−38	−70	8
	YH	−18	−75	39	−45	−30	24	−37	−39	59	−26	−48	47	−14	−47	52*	−14	−16	39	−42	−60	9
	Mean	−11	−79	30	−38	−31	19	−27	−43	52	−25	−55	50	−14	−46	48	−10	−23	39	39	−60	1
Right	AS	10	−78	29	35	−29	15*	30	−39	43	27	−59	43	11	−47	46	—	—	—	39	−51	−3
	EC	14	−70	24	37	−33	16	30	−41	45	35	−59	47	12	−37	38*	12	−26	35	45	−60	−4
	JC	17	−86	28	—	—	—	28	−47	56	25	−63	41*	15	−51	46*	12	−32	39	34	−67	−1
	JS	12	−72	24	37	−33	19	28	−45	57*	19	−61	46	15	−47	45	2	−18	46*	—	—	—
	KL	15	−78	30	34	−30	17*	31	−46	52	32	−51	47	7	−51	51*	11	−33	42	37	−59	3
	MB	11	−80	33	40	−29	18	33	−51	59	26	−54	48*	13	−51	51*	15	−21	40	38	−61	2
	MN	11	−74	37	—	—	—	28	−36	52**	22	−47	46**	—	—	—	11	−21	40**	41	−62	2
	PK	22	−78	32	32	−30	21	19	−42	52	24	−53	59*	5	−51	50**	11	−29	43*	40	−55	6
	SD	13	−81	29	37	−28	19	31	−43	48*	—	—	—	16	−49	48	13	−20	40	39	−66	5
	VC	10	−73	29	37	−31	15*	21	−40	47*	22	−52	48*	—	—	—	13	−24	36	37	−63	4
	YH	19	−81	30	40	−35	20	24	−42	45	26	−63	51	3	−53	47*	11	−22	43	40	−58	2
	Mean	14	−77	30	37	−31	18	28	−43	48	26	−56	48	11	−49	47	11	−25	40	−39	−62	5

Note: The table shows the coordinates of the maxima of each ROI for the statistical contrast (EC–EI). All maxima were significant at $P < 0.05$ (whole brain, Bonferroni corrected), with exception of "*" ($P < 0.001$, uncorrected) and "**" ($P < 0.005$, uncorrected).

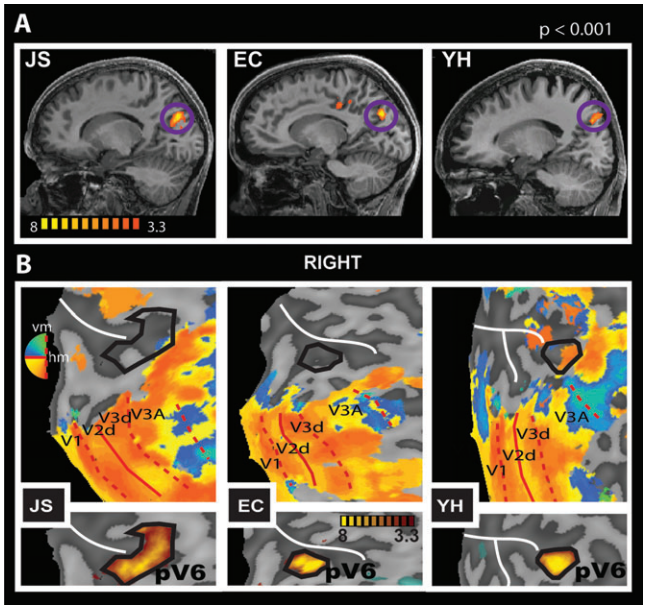

Figure 2. Differential response to EC stimuli in the POS. (*A*) Sagittal slices of the right hemisphere of 3 participants (JS, EC, and YH) showing the localization of a region selectively responsive to EC stimulation in the fundus of the POS. *T* values are color coded (see color bar). (*B*) Retinotopic maps (upper panels) and regions selectively responsive to EC (lower panels), overlaid onto flattened representations of the right occipital lobes of the same 3 participants. Retinotopic maps were obtained with narrow-field (24°) stimulation and show the demarcation of dorsal visual areas V1–V3A. The location of the POS region defined by sensitivity to EC stimuli, taken from the lower panel, is also shown (solid black line) on each retinotopic map. Red thin lines show the borders between visual areas (dashed: vertical meridian [vm]; continuous: horizontal meridian [hm]). Representations of different parts of the visual field are color coded (see color wheel; all activations thresholded at $P < 0.01$). The white line marks the POS.

also sensitive to optic flow and is in the same anatomical vicinity but has an independent contralateral hemifield representation. We highlight that the definition of V3A and pV6 was based on an independent localizer (retinotopic mapping). Beta values from pV6 were extracted from all the hemispheres where it was possible to demarcate this area retinotopically (7 with wide-field mapping and 1 with standard small field mapping—data from one hemisphere was excluded because of an unusual large, negative effect of EI in pV6). The responses from V3A were extracted from the 8 same hemispheres in which it was possible to define pV6 retinotopically. Results are shown in Figure 3*B*. The EI/EC coefficient in pV6 is 0.52 ± 0.08; therefore, in pV6, EC evokes double the response of EI, showing a strong preference for optic flow stimulation that is consistent with egomotion. In contrast, the EI/EC coefficient in area V3A is 0.95 ± 0.03, meaning that this area responds about equally well to both kinds of optic flow pattern.

Differential responses to EC stimuli are also observed in the POS with smaller field stimulation (20°) as we show in Supplementary Figure 2. This could be reliably identified in 7/8 hemispheres using a $P < 0.001$ threshold, showing that this protocol could be used, without wide-field stimuli, as a general procedure for identifying this egomotion-sensitive region in the POS—an approach similar to the contrast between optic flow and motion noise described by Pitzalis et al. (2009) for the identification of human V6.

Posterior Insula: PIVC

The contrast (EC–EI) also showed significant activity in the posterior/dorsal extreme of the insula (Figs 1 and 4, green, and Table 1), sometimes extending into the parietal operculum. We observed differential activity in this region bilaterally and consistently across subjects (18/22 hemispheres; Table 1). The mean coordinates of this region are $x = 37$, $y = -31$, $z = 18$

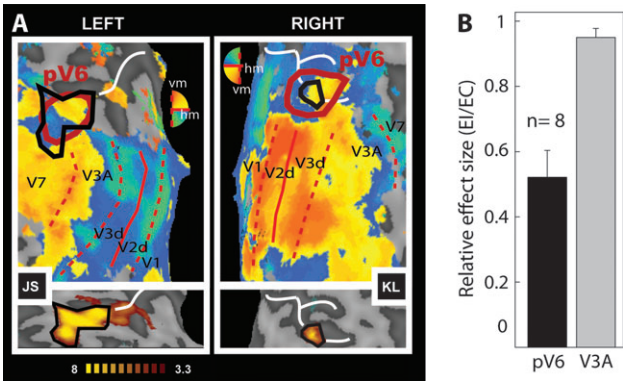

Figure 3. Sensitivity of putative human V6 to EC visual stimulation. (*A*) Retinotopic maps (upper panels) and regions selectively responsive to EC (lower panels) overlaid onto flattened representations of the occipital lobes of 2 participants (JS and KL). Retinotopic maps were obtained with wide-field (70°) stimulation and show dorsal visual areas and the demarcation of human pV6 based on retinotopic criteria (thick red line). pV6 has a full hemifield representation with the upper quadrant represented nearer to V2 and the lower quadrant nearer to V3A (note that the color key is vertically reversed for the 2 hemispheres, in *BrainVoyager* convention). pV6 as defined by sensitivity to EC stimuli, from the lower panel, is also shown (solid black line) on each retinotopic map. Thin red lines show the borders between visual areas (dashed: vertical meridian [vm]; continuous: horizontal meridian [hm]). Representations of different parts of the visual field are color coded (see color wheel [note that colors have opposite dorsal–ventral meanings in the 2 hemispheres]; all activations thresholded at $P < 0.01$). The white line marks the POS. (*B*) Relative response magnitudes, in terms of the average coefficient of beta values (EI/EC), in areas V3A and pV6 ($n = 8$ hemispheres). Bars represent the mean coefficients across participants ± standard error of the mean.

(right) and $x = -38$, $y = -31$, $z = 19$ (left). This location is in line with the description of human PIVC identified with galvanic stimulation of the mastoids and caloric stimulation of the ear canal (Bottini et al. 1994; Bucher et al. 1998; Fasold et al. 2002; Dieterich, Bense, Lutz, et al. 2003; Indovina et al. 2005; Eickhoff, Amunts, et al. 2006).

Thus, PIVC, which was already known to be polysensory and to receive visual input, can be localized in humans with EC visual stimuli. The relationship between this finding and other reports of visual activity in PIVC will be considered in the Discussion.

Parietal Regions—Area p2v and Precuneus

In addition to pVIP, we localized 2 areas in the parietal lobe that are more responsive to EC than EI stimuli. They are shown in Figure 5. One is in the dorsal portion of the postcentral sulcus, in Brodmann area (BA) 5, or area 5L/7Pc of Scheperjans et al. (2008; Figs 1, 5*A*,*B*, white circles). This area appears to be the same as a region activated by Lobel et al. (1998) in a study of galvanic vestibular stimulation, which may be homologous to macaque vestibular area 2v; therefore, we refer to it as putative human area 2v or p2v (see Discussion). The other region is more medial, in the precuneus, in the ascending ramus of the cingulate sulcus, in BA7 or 5M (Figs 1, 5*A*,*B*, red circles).

Area p2v was present in 20/22 hemispheres and had mean coordinates $x = 28$, $y = -43$, $z = 48$ (right) and $x = -27$, $y = -43$, $z = 52$ (Table 1). The activation in the precuneus was present in 19/22 hemispheres, with coordinates $x = 11$, $y = -49$, $z = 47$ (right) and $x = -14$, $y = -46$, $z = 48$ (Table 1). Activity corresponding to frontal area 3aNv was not seen. Thus, vestibular areas PIVC and p2v can be identified with EC visual stimuli but area 3aNv apparently cannot.

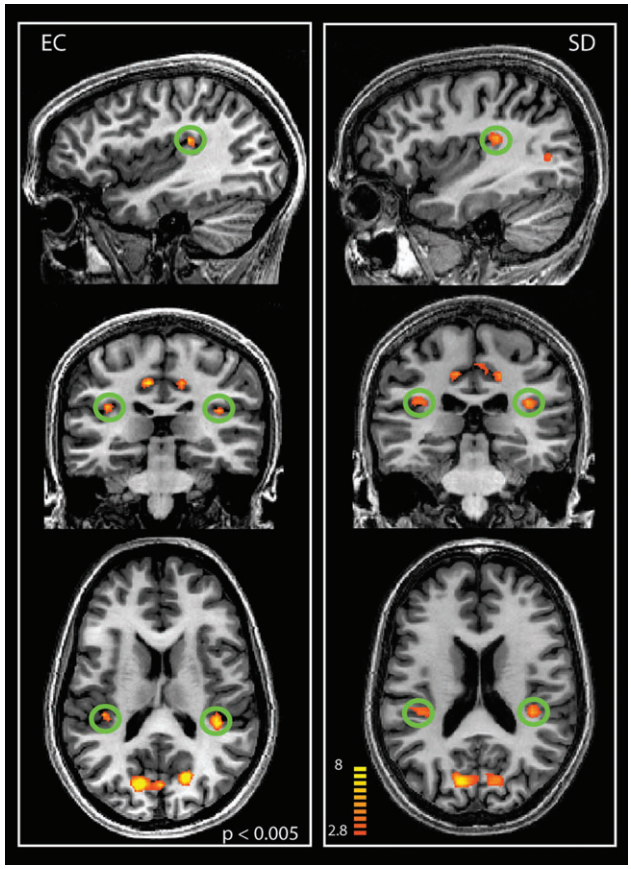

Figure 4. Activation of human PIVC with EC visual stimulation. The figure shows the regions selectively responsive to EC stimuli in sagittal, coronal, and axial slices of the brains of 2 individuals. The green circles indicate the localization of the PIVC. *T* values are color coded (see color bar).

Response to EI Stimuli in Areas Differentially Responsive to EC Stimuli

To determine the relative effect of EC and EI stimuli in each of the differentially active areas, we extracted beta values for all voxels in each of these regions and plotted the averaged coefficient of EI/EC as we did in Figure 3*B*. It should be noted that here, in contrast to Figure 3*B*, the ROI definition was itself obtained with the statistical contrast (EC–EI). This ROI definition is not independent and could introduce a bias in the results toward EC stimuli. However, we considered that it is nevertheless useful for comparing the degree of specificity for EC stimuli across the various brain regions. Beta values were extracted from ROIs centered at the peak coordinates (Table 1) of the activation (see Materials and Methods; data from the right PIVC of one participant was excluded because of an unusual large, negative coefficient of –16). Results are presented in Figure 6. Coefficients in all ROIs are smaller than 0.5, highlighting the fact that EC stimuli had, at least, 2 times the effect of EI stimuli. However, values in pV6 and pVIP (0.4 ± 0.03 and 0.31 ± 0.08, respectively) were higher than those in the other regions (PIVC = 0.18 ± 0.05; CSv = 0.15 ±.04; p2v = –0.02 ± 0.1; Pc = –0.34 ± .20), in particular p2v and Pc, where negative values indicate that the EI had no or negative effects in those regions. These results suggest that regions such as pV6 and pVIP, which are visual motion areas, will respond to EI stimuli, but have a preferential response to EC stimuli, possibly being involved in extracting egomotion-related information from

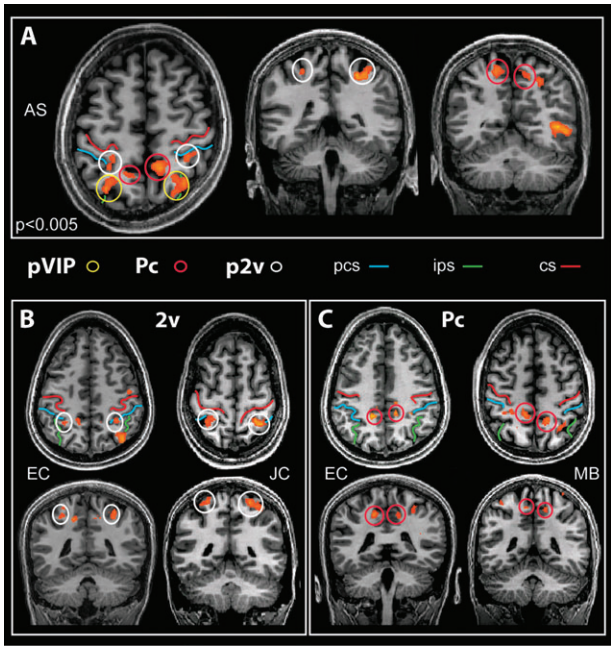

Figure 5. Parietal regions activated by EC stimuli. (*A*) Slices from the brain of a representative participant, showing the location of all 3 parietal regions (p2v, pVIP, and Pc) in the same axial slice (left) and in coronal view. (*B*, *C*) Location of areas p2v (*B*) and Pc (*C*) in slices from 2 other participants. The 3 regions are identified with colored circles as in other figures. Three sulci are marked by colored lines: central sulcus (cs), intraparietal sulcus (ips), and postcentral sulcus (pcs). *T* values are color coded as in Figure 3.

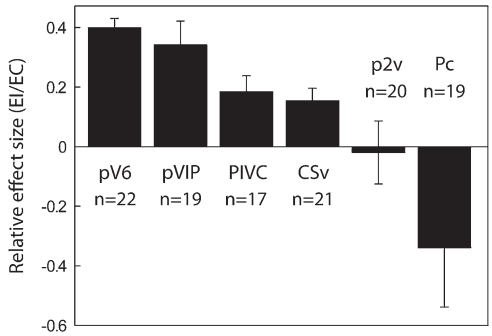

Figure 6. Average coefficient of beta values (EI/EC) in areas pV6, pVIP, PIVC, CSv, p2v, and Pc. Beta values were extracted from functionally defined ROIs (see Materials and Methods and Results). Bars represent the mean coefficients ± SEM across runs and participants (*n* indicates number of hemispheres).

motion patterns. However, vestibular areas p2v and PIVC, and parietal areas CSv and Pc, have either a weak or absent response to EI stimuli. These regions do not respond to patches of coherent flow irrespective of context but only when the overall flow stimulus is consistent with egomotion. Possibly they are more closely related to the representation of egomotion than pV6 and pVIP. In the case of Pc, the mean response to EI was actually negative, giving a negative (EI/EC) coefficient, although the large variance and the nonindependence of the ROI definition must be borne in mind.

It should be noted that the values obtained with the independent (Fig. 3*B*) and nonindependent functional (Fig. 6) definitions of pV6 are 0.52 ± 0.08 and 0.4 ± 0.03, respectively. Therefore, we think that the bias introduced by the use of a nonindependent functional ROI definition is real in quantitative terms but insufficient to invalidate the qualitative conclusions we have drawn from Figure 6.

Possible Effects of Eye and Head motion

A possible explanation of differential sensitivity to EC stimuli is that they might elicit movements of the eyes and/or head that are greater for EC than EI stimuli, and this might lead to artefactual differences. However, because the stimuli were fixated at a centre of expansion in both cases, differential movements are unlikely. If anything, multiple patches are expected to produce greater movements because of the risk of exploring different patches. We established empirically that head motion was no greater during EC trials than EI trials (see Supplementary Fig. 3).

Discussion

We have demonstrated differential sensitivity of several human cortical regions to egomotion-compatible (EC) visual stimulation. We suggest that these areas, some of which are traditionally more strongly associated with vestibular than visual activity, may be involved in the extraction of visual cues for the processing of egomotion.

Involvement of V6 in Optic Flow and Egomotion

We have shown a differential activation to EC stimuli, consistent across subjects, in the dorsal region of the POS. With retinotopic mapping, we have shown a hemifield representation at a broadly overlapping location that we refer to as pV6. Because pV6 is responsive to optic flow that has a single centre of expansion but much less responsive to coherent flow stimuli with several centers of expansion, we suggest that pV6 is involved in the extraction of optic flow cues for egomotion processing.

A few previous studies have shown activation in parieto-occipital areas when participants experienced vection, but none of them have linked this activation to a region containing a retinotopic representation (pV6). When comparing self-motion (vection) versus object motion (no vection), Kovács et al. (2008) found a focus of activation in the POS, extending to the cuneus and precuneus. The peak coordinates of their group analysis ($x = -12$, $y = -62$, $z = 33$) are similar to those we report for human pV6 in the x- and z-axes but more anterior. It is possible that the more posterior part of their activation may correspond to pV6. Brandt et al. (1998) also showed activations with circular rotation that induced vection, at a location ($x = 6$, $y = -82$, $z = 27$) similar to pV6.

As noted in the Results section, the variable location of our pV6 might raise some doubt as to whether it corresponds cleanly to V6 of Pitzalis et al. (2006). However, 2 factors lead us to conclude that both studies probably identify the same area. First, in a recent study, Pitzalis et al. (2009) identified human V6 retinotopically and showed that this area responds to coherent optic flow fields but not to incoherent motion. They do not report any other area in the vicinity with the same functional preference and conclude that their stimuli could be used as functional localizer of human V6. However, it is expected that if the region we identify in the POS were other than V6, Pitzalis et al. (2009) would have identified it in their study since it is selective for optic flow. We therefore take this result to

support the view that the region that we define as pV6 probably is, indeed, human V6.

Second, close inspection of the data reveals that the location of V6 as defined by Pitzalis et al. (2006, 2009) also varies across subjects. In their original study, Pitzalis et al. (2006) defined human V6 as a complete hemifield medial to V3 and V3A and anterior to peripheral V2. However, the location of the region identified as V6 in their later study (Pitzalis et al. 2009) shows some variability (see their Fig. 5). In some participants (e.g., their Subject 7), it is located close to the border between V3A and V7; in others (e.g., Subject 10) it is close to V2, not sharing a border with V3A. The location of pV6, as we retinotopically define it, shows the same variability. In most cases, it is medially adjacent to the end of V3A; sometimes, it appears to about V3d as closely as V3A, meeting the most eccentric representation of V2; in a few cases, it is nearer to the V3A/V7 border. The same kind of variability is observed in the POS activation identified with EC stimulation. This variability may reflect genuine individual differences. Alternatively, it might reflect apparent differences resulting from the extent to which V2, V3, and V3A are successfully mapped into the periphery, which influences where the "ends" of these areas appear to lie relative to pV6. The crucial point is that variability is correlated across the 2 types of measurement: when the retinotopic map is closer to V7, so is the EC flow-related activity. In all the cases in which we identify a complete hemifield located in POS medially to V3A, the response of this region was selective for EC stimuli, it overlapped with the cluster identified with the (EC–EI) statistical contrast, and there was no other independent hemifield representation in the vicinity that was a better candidate for V6.

A possibility to be considered is that the POS region identified by our procedure might be the human homologue of macaque V6A, rather than V6. In macaques, V6 and V6A are adjacent, V6A being located more dorsally but still within the POS. In terms of response properties, the main differences are that 1) most V6 cells are visually responsive whereas many V6A cells are not, 2) receptive fields are larger in V6A, and 3) unlike V6, there is no clear retinotopic map in V6A (Galletti, Fattori, Kutz, et al. 1999). Both areas have a high level of direction specificity among visually responsive neurons, and both are potential candidates for involvement in optic flow. In our study, the assertion that the region activated with EC stimuli in the POS represents V6 rests on the fact that, in the cases where we were able to apply both methods in the same hemisphere, our EC-defined area overlaps heavily with a region containing a retinotopic map (the region that we defined as pV6). Moreover, when we defined pV6 retinotopically and then compared responses to EC and EI stimuli within it, we found a strong preference for EC stimuli (Fig. 3*B*). Nonetheless, because the 2 areas are small and adjacent in macaques and because our retinotopic maps are variable and sometimes ill defined, we cannot rule out the possibility that our pV6 includes human V6A. There may, of course, be important species differences than make it inappropriate to map activity onto counterparts of V6 and V6A.

In our study, we show that pV6 is differentially responsive to flow fields that have a single centre of expansion. Note that both of our stimuli contain coherent motion; even in the EI condition, each coherent patch subtends 19 × 19°. In view of these results and previous associations with vection, a plausible interpretation of the differential sensitivity of pV6 to a single flow patch is that this region selectively encodes visual stimuli that are consistent with egomotion. This is the explanation advanced by Wall and Smith (2008) to explain similar results obtained in pVIP and CSv. If pV6 is the homologue of macaque V6, there are 2 other pieces of evidence that make it suitable for the analysis of optic flow and egomotion: 1) V6 contains a representation of the contralateral visual field that extends up to 80°, in which the centre is not magnified relative to the periphery (shown by Galletti, Fattori, Gamberini, et al. 1999, in macaque; confirmed in humans by Pitzalis et al. 2006; Stenbacka and Vanni 2007) and 2) V6 is reciprocally connected to visual areas thought to be involved in egomotion perception, such as MST and VIP (Shipp et al. 1998; Galletti et al. 2001).

Activation of Vestibular Areas PIVC and p2v by Optic Flow

Another significant finding is that human PIVC can be activated differentially by EC optic flow stimuli (demonstrated in 18/20 hemispheres). In macaque, PIVC neurons are multisensory, responding to vestibular, somatosensory, and optokinetic stimulation (Grüsser et al. 1990a, 1990b). Previous studies in humans have localized this area using fMRI or PET with caloric stimulation of the ear canal or galvanic stimulation of the mastoids (Bottini et al. 1994; Bucher et al. 1998; Fasold et al. 2002; Dieterich, Bense, Lutz, et al. 2003; Indovina et al. 2005; Eickhoff, Weiss, et al. 2006). The centre of the activation we observe in the posterior insula is located close to the centre of OP2 (right: $x = 37$, $y = -25$, $z = 22$; left: $x = -37$, $y = -267$, $z = 23$; MNI coordinates, Eickhoff, Amunts, et al. 2006), the cytoarchitectonic region that Eickhoff, Weiss, et al. (2006) identified, with galvanic vestibular stimulation, as the homologous to macaque PIVC. Previous studies have demonstrated visual activity in this vicinity using optic flow stimuli, although there is some uncertainty about the location of visual activity in relation to PIVC as identified with vestibular stimuli. Using optic flow stimuli (Sunaert et al. 1999) obtained activity at a location similar to ours but were cautious about defining it as PIVC, referring to it instead as PIC and suggesting that it might be a homologue of monkey VPS, which is located slightly more posteriorly and dorsally with respect to PIVC (Guldin and Grüsser 1998). Conceivably, therefore, our activity is not in PIVC but in a neighboring area such as the homologue of VPS. To resolve this issue would probably require careful comparison of visual and vestibular activity in the same study. Meanwhile, we refer to our visual activation as PIVC based on its similarity of location to PIVC in previous studies that used vestibular stimulation, fMRI, and cytoarchitectonic mapping (Eickhoff, Amunts, et al. 2006; Eickhoff, Weiss, et al. 2006).

Superficially, our results conflict with previous studies that have shown deactivations in PIVC when rotation stimuli are compared with random motion (Brandt et al. 1998) or when periods of vection are compared with periods of perceived object motion (Kleinschmidt et al. 2002). Deutschländer et al. (2002) showed that the combination of visual and vestibular stimulation activates visual and vestibular areas (including PIVC) to a lesser extent than unisensory stimulation, suggesting a reciprocal, inhibitory vestibular–visual interaction. However, in agreement with our results, in a study comparing coherent with incoherent motion, Antal et al. (2008) showed activation in the planum temporale/parietal operculum region, which seems to include PIVC. Neither in our study nor in that of Antal et al. (2008) did participants experience vection. It could be that PIVC responds well to EC optic flow in the absence of

vection but that the onset of vection reduces or eliminates this response. Thus, in the study of Brandt et al. (1998), which was designed to compare vection with no vection, vection might have reduced the PIVC response to a rotating stimulus below that elicited by random motion, whereas with no vection, rotation might have yielded a larger response than random motion. Studies looking at the interaction of EC and EI visual stimulation with galvanic or caloric stimulation will be necessary to differentiate the possibilities.

We also observed 3 parietal regions that were more responsive to EC than EI stimuli: pVIP, in the anterior intraparietal sulcus; p2v, in the dorsal margin of the postcentral sulcus (BA5); and a part of the precuneus (medial BA7), posterior to the dorsal margin of the ascending ramus of the cingulate sulcus. The activity in pVIP confirms previous findings (Bremmer et al. 2001; Wall and Smith 2008), suggesting that this area plays a key role in the extraction of visual cues to egomotion. We suggest that the region in BA5, termed p2v, corresponds to the human homologue of area 2v. We do so for the following reasons: 1) macaque 2v is a multisensory area, containing neurons that respond to vestibular and optokinetic stimulation (Büttner and Buettner 1978), and 2) in humans, activations in p2v have been observed with stimulation of neck muscles and with galvanic vestibular stimulation (Lobel et al. 1998; Fasold et al. 2008). PIVC and area 2v are interconnected (Brandt and Dieterich 1999), and both have projections to the vestibular nuclei (Akbarian et al. 1994). These areas, along with area 3aV in the central sulcus, form the vestibular cortical system (Guldin and Grüsser 1998; Brandt and Dieterich 1999). Our study shows that it is possible to localize much of this vestibular network using exclusively visual stimulation.

Possible Involvement of Precuneus in Egomotion

The precuneus (BA7) is involved in functions related to visuospatial imagery and orientation, episodic memory retrieval, and self-related processes (see Cavanna and Trimble [2006], for a review). Notably, it is involved in the retrieval of an event or person in a spatial context (Burgess et al. 2001), for which it is necessary to have access to a spatial representation of the world. It has recently been shown that part of the precuneus is active when subjects have to update the spatial location of objects taking into account a self-displacement (Wolbers et al. 2008). The precuneus has been associated with perceiving global motion (Bartels et al. 2008), and most directly, vestibular disturbance has been reported in at least one patient with a circumscribed lesion in the precuneus (Wiest et al. 2004).

In macaques, medial BA7 connects to several regions responsive to egomotion, including MST, VIP, the POS, the cingulate sulcus (where CSv is located in humans), and the caudal parietal operculum possibly including PIVC (Cavada and Goldman-Rakic 1989; Leichnetz 2001). Therefore, given the anatomical and functional evidence, we suggest that our area in the precuneus may be part of the visuovestibular circuit of areas involved in the processing of egomotion.

Conclusion

In conclusion, using exclusively visual stimulation, we have shown the differential activation by egomotion-compatible stimuli of several visual and vestibular regions including pV6, pVIP, CSv, area p2v, PIVC, and a portion of the precuneus. These areas are all potentially implicated in encoding the motion of the body through space. Areas pV6 and pVIP have a strong preference for EC optic flow, although EI optic flow patterns also elicit a significant response. On the other hand, vestibular areas p2v and PIVC, and parietal areas CSv and Pc, respond only when the stimulus is consistent with egomotion, suggesting that these areas are placed higher up in the processing hierarchy and possibly receive inputs from motion areas, such as pV6 and pVIP. We also suggest that our methodology could potentially be used to localize vestibular areas PIVC and p2v without the need for vestibular stimuli.

Supplementary Material

Supplementary Figures 1–3 can be found at: http://www.cercor.oxfordjournals.org/.

Funding

Wellcome Trust (to A.T.S.). Open Access charges were also paid by the Wellcome Trust.

Notes

Conflict of Interest: None declared.

Address correspondence to email: a.t.smith@rhul.ac.uk.

References

Akbarian S, Berndl K, Grüsser OJ, Guldin W, Pause M, Schreiter U. 1988. Responses of single neurons in the parietoinsular vestibular cortex of primates. Ann N Y Acad Sci. 545:187–202.

Akbarian S, Grüsser OJ, Guldin WO. 1994. Corticofugal connections between the cerebral cortex and brainstem vestibular nuclei in the macaque monkey. J Comp Neurol. 339:421–437.

Antal A, Baudewig J, Paulus W, Dechent P. 2008. The posterior cingulate cortex and planum temporale/parietal operculum are activated by coherent visual motion. Vis Neurosci. 25:17–26.

Bartels A, Zeki S, Logothetis NK. 2008. Natural vision reveals regional specialization to local motion and to contrast-invariant, global flow in the human brain. Cereb Cortex. 18:705–717.

Bottini G, Sterzi R, Paulesu E, Vallar G, Cappa SF, Erminio F, Passingham RE, Frith CD, Frackowiak RS. 1994. Identification of the central vestibular projections in man: a positron emission tomography activation study. Exp Brain Res. 99:164–169.

Brandt T, Bartenstein P, Janek A, Dieterich M. 1998. Reciprocal inhibitory visual-vestibular interaction—visual motion stimulation deactivates the parieto-insular vestibular cortex. Brain. 121:1749–1758.

Brandt T, Dieterich M. 1999. The vestibular cortex: its locations, functions and disorders. Ann N Y Acad Sci. 871:293–312.

Bremmer F, Schlack A, Shah N, Zafiris O, Kubischik M, Hoffmann K-P, Zillies K, Fink G. 2001. Polymodal motion processing in posterior parietal and premotor cortex: a human fMRI study strongly implies equivalencies between humans and monkeys. Neuron. 29:287–296.

Bucher S, Dieterich M, Weismann M, Weiss A, Zink R, Yousry T, Brandt T. 1998. Cerebral functional magnetic resonance imaging of vestibular, auditory and nociceptive areas during gavanic stimulation. Ann Neurol. 44:120–125.

Burgess N, Maguire EA, Spiers HJ, O'Keefe J. 2001. A temporoparietal and prefrontal network for retrieving the spatial context of lifelike events. Neuroimage. 14:439–453.

Büttner U, Buettner U. 1978. Parietal cortex (2v) neuronal activity in the alert monkey during natural vestibular and optokinetic stimulation. Brain Res. 153:392–397.

Büttner U, Henn V. 1981. Circularvection: psychophysics and single-unit recordings in the monkey. Ann N Y Acad Sci. 374:274–283.

Cavada C, Goldman-Rakic PS. 1989. Posterior parietal cortex in rhesus monkey: I. parcellation of areas based on distinctive limbic and sensory corticocortical connections. J Comp Neurol. 287:393–421.

Cavanna A, Trimble M. 2006. The precuneus: a review of its functional anatomy and behavioural correlates. Brain. 129:564.

de Jong BM, van der Graaf FH, Paans AM. 2001. Brain activation related to the representations of external space and body scheme in visuomotor control. Neuroimage. 14:1128–1135.
Deichmann R, Schwarzbauer C, Turner R. 2004. Optimisation of the 3D MDEFT sequence for anatomical brain imaging: technical implications at 1.5 and 3 T. Neuroimage. 21:757–767.
Deutschländer A, Bense S, Stephan T, Schwaiger M, Brandt T, Dieterich M. 2002. Sensory system interactions during simultaneous vestibular and visual stimulation in PET. Hum Brain Mapp. 16:92–103.
Dieterich M, Bense S, Lutz S, Drzezga A, Stephan T, Bartenstein P, Brandt T. 2003. Dominance for vestibular cortical function in the non-dominant hemisphere. Cereb Cortex. 13:994–1007.
Dieterich M, Bense S, Stephan T, Yousry TA, Brandt T. 2003. fMRI signal increases and decreases in cortical areas during small-field optokinetic stimulation and central fixation. Exp Brain Res. 148:117–127.
Duffy CJ, Wurtz RH. 1991a. Sensitivity of MST neurons to optic flow stimuli. II. Mechanisms of response selectivity revealed by small-field stimuli. J Neurophysiol. 65:1346–1359.
Duffy CJ, Wurtz RH. 1991b. Sensitivity of MST neurons to optic flow stimuli. I. A continuum of response selectivity to large-field stimuli. J Neurophysiol. 65:1329–1345.
Duffy CJ, Wurtz RH. 1995. Responses of monkey MST neurons to optic flow stimuli with shifted centers of motion. J Neurosci. 15:5192–5208.
Duhamel JR, Colby CL, Goldberg ME. 1998. Ventral intraparietal area of the macaque: congruent visual and somatic response properties. J Neurophysiol. 79:126–136.
Eickhoff SB, Amunts K, Mohlberg H, Zilles K. 2006. The human parietal operculum. II. Stereotaxic maps and correlation with functional imaging results. Cereb Cortex. 16:268–279.
Eickhoff SB, Weiss PH, Amunts K, Fink GR, Zilles K. 2006. Identifying human parieto-insular vestibular cortex using fMRI and cytoarchitectonic mapping. Hum Brain Mapp. 27:611–621.
Engel SA, Rumelhart DE, Wandell BA, Lee AT, Glover GH, Chichilnisky EJ, Shadlen MN. 1994. fMRI of human visual cortex. Nature. 369:525.
Fasold O, Heinau J, Trenner MU, Villringer A, Wenzel R. 2008. Proprioceptive head posture-related processing in human polysensory cortical areas. Neuroimage. 40:1232–1242.
Fasold O, von Brevern M, Kuhberg M, Ploner CJ, Villringer A, Lempert T, Wenzel R. 2002. Human vestibular cortex as identified with caloric stimulation in functional magnetic resonance imaging. Neuroimage. 17:1384–1393.
Fattori P, Galletti C, Battaglini P. 1992. Parietal neurons encoding visual space in a head-frame of reference. Boll Soc Ital Biol Sper. 68:663–670.
Galletti C, Battaglini PP, Fattori P. 1991. Functional properties of neurons in the anterior bank of the parieto-occipital sulcus of the macaque monkey. Eur J Neurosci. 3:452–461.
Galletti C, Fattori P, Battaglini PP, Shipp S, Zeki S. 1996. Functional demarcation of a border between areas V6 and V6A in the superior parietal gyrus of the macaque monkey. Eur J Neurosci. 8:30–52.
Galletti C, Fattori P, Gamberini M, Kutz DF. 1999. The cortical visual area V6: brain location and visual topography. Eur J Neurosci. 11:3922–3936.
Galletti C, Fattori P, Kutz DF, Gamberini M. 1999. Brain location and visual topography of cortical area V6A in the macaque monkey. Eur J Neurosci. 11:575–582.
Galletti C, Gamberini M, Kutz DF, Fattori P, Luppino G, Matelli M. 2001. The cortical connections of area V6: an occipito-parietal network processing visual information. Eur J Neurosci. 13:1572–1588.
Gibson JJ. 1950. The perception of the visual world. Boston: Houghton Mifflin.
Grüsser OJ, Pause M, Schreiter U. 1990a. Localization and responses of neurones in the parieto-insular vestibular cortex of awake monkeys (Macaca fascicularis). J Physiol. 430:537–557.
Grüsser OJ, Pause M, Schreiter U. 1990b. Vestibular neurones in the parieto-insular cortex of monkeys (Macaca fascicularis): visual and neck receptor responses. J Physiol. 430:559–583.
Gu Y, Angelaki DE, DeAngelis GC. 2008. Neural correlates of multisensory cue integration in macaque MSTd. Nat Neurosci. 11:1201–1210.
Gu Y, DeAngelis GC, Angelaki DE. 2007. A functional link between area MSTd and heading perception based on vestibular signals. Nat Neurosci. 10:1038–1047.
Gu Y, Watkins PV, Angelaki DE, DeAngelis GC. 2006. Visual and nonvisual contributions to three-dimensional heading selectivity in the medial superior temporal area. J Neurosci. 26:73–85.
Guldin W, Grüsser O-J. 1998. Is there a vestibular cortex? Trends Neurosci. 21:254–259.
Indovina I, Maffei V, Bosco G, Zago M, Macaluso E, Lacquaniti F. 2005. Representation of visual gravitational motion in the human vestibular cortex. Science. 416–418.
Kikuchi M, Naito Y, Senda M, Okada T, Shinohara S, Fujiwara K, Hori S-Y, Tona Y, Yamazaki H. 2009. Cortical activation during optokinetic stimulation – an fMRI study. Acta Otolarungology. 129:140–143.
Kleinschmidt A, Thilo KV, Büchel C, Gresty MA, Bronstein AM, Frackowiak RSJ. 2002. Neural correlates of visual-motion perception as object- or self-motion. Neuroimage. 16:873–882.
Kovács G, Raabe M, Greenlee MW. 2008. Neural correlates of visually induced self-motion illusion in depth. Cereb Cortex. 18:1779–1787.
Leichnetz GR. 2001. Connections of the medial posterior parietal cortex (area 7m) in the monkey. Anat Rec. 263:215–236.
Lobel E, Kleine JF, Bihan DL, Leroy-Willig A, Berthoz A. 1998. Functional MRI of galvanic vestibular stimulation. J Neurophysiol. 80:2699–2709.
Morrone MC, Tosetti M, Montanaro D, Fiorentini A, Cioni G, Burr DC. 2000. A cortical area that responds specifically to optic flow, revealed by fMRI. Nat Neurosci. 3:1322–1328.
Page W, Duffy C. 2003. Heading representation in MST: sensory interactions and population encoding. J Neurophysiol. 89:1994–2013.
Peuskens H, Sunaert S, Dupont P, Van Hecke P, Orban GA. 2001. Human brain regions involved in heading estimation. J Neurosci. 21:2451–2461.
Pitzalis S, Galletti C, Huang R-S, Patria F, Committeri G, Galati G, Fattori P, Sereno MI. 2006. Wide-field retinotopy defines human cortical visual area V6. J Neurosci. 26:7962–7963.
Pitzalis S, Sereno MI, Committeri G, Fattori P, Galati G, Patria F, Galletti C. Forthcoming 2009. Human V6: the medial motion area. Cereb Cortex.
Saito H, Tanaka K, Isono H, Yasuda M, Mikami A. 1989. Directionally selective responses of cells in the middle temporal area (MT) of the macaque monkey to the movement of equiluminous opponent color stimuli. Exp Brain Res. 75:1–14.
Schaafsma SJ, Duysens J. 1996. Neurons in the ventral intraparietal area of awake macaque monkey closely resemble neurons in the dorsal part of the medial superior temporal area in their responses to optic flow patterns. J Neurophysiol. 76:4056–4068.
Scheperjans F, Hermann K, Eickhoff SB, Amunts K, Schleicher A, Zilles K. 2008. Observer-independent cytoarchitectonic mapping of the human superior parietal cortex. Cereb Cortex. 18:846–867.
Sereno MI, Dale AM, Reppas JB, Kwong KK, Belliveau JW, Brady TJ, Rosen BR, Tootell RB. 1995. Borders of multiple visual areas in humans revealed by functional magnetic resonance imaging. Science. 268:889–893.
Shipp S, Blanton M, Zeki S. 1998. A visuo-somatomotor pathway through superior parietal cortex in the macaque monkey: cortical connections of areas V6 and V6A. Eur J Neurosci. 10:3171–3193.
Simon O, Mangin JF, Cohen L, Le Bihan D, Dehaene S. 2002. Topographical layout of hand, eye, calculation, and language-related areas in the human parietal lobe. Neuron. 33:475–487.
Stenbacka L, Vanni S. 2007. Central luminance flicker can activate peripheral retinotopic representation. Neuroimage. 34:342–348.
Sunaert S, VanHecke P, Marchal G, Orban GA. 1999. Motion-responsive regions of the human brain. Exp Brain Res. 127:355–370.
Wall M, Smith A. 2008. The representation of egomotion in the human brain. Curr Biol. 18:191–194.
Warren WH, Hannon DJ. 1988. Direction of self-motion is perceived from optical flow. Nature. 336:162–163.
Wiest G, Zimprich F, Prayer D, Czech T, Serles W, Baumgartner C. 2004. Vestibular processing in human paramedian precuneus as shown by electrical cortical stimulation. Neurology. 62:473–475.
Wolbers T, Hegarty M, Buchel C, Loomis J. 2008. Spatial updating: how the brain keeps track of changing object locations during observer motion. Nat Neurosci. 11:1223–1230.
Zhang T, Heuer HW, Britten KH. 2004. Parietal area VIP neuronal responses to heading stimuli are encoded in head-centered coordinates. Neuron. 42:993–1001.